

Supporting Information

Horne *et al.* 10.1073/pnas.0801135105

SI Text

Structural Characteristics of α/β -Peptide 7. As discussed in the main text, a canonical coiled coil is characterized by hydrophobic residues that are alternatively three and four residues apart in primary sequence (i.e., a 3-4-3-4-3-4 repeat). The seven residues in each heptad are typically assigned the letters *abcdefg*, with hydrophobic core residues denoted as *a* and *d*. In a parallel helix bundle fold, the interface between helices is characterized by alternating layers composed of *a* position residues (“*a*-layers”) and *d* position residues (“*d*-layers”). This is the case for the GCN4-pLI α -peptide (**1**) as well as α/β -peptide derivatives **2-4** (i.e., the same sequence positions comprise the hydrophobic cores of **1-4**). In α/β -peptide **7**, however, there is a break in the heptad repeat of hydrophobic residues that comprise the core of the helix bundle. Specifically, there is a formal deletion of four residues from the 3-4-3-4-3-4 repeat, leading to a local 3-4-3-3-4 pattern of core residues (Fig. S4). In natural coiled-coil structures, this type of heptad discontinuity is referred to a “helical stammer” (**1**). The change in hydrophobic core packing between **4** and **7** is discussed in greater detail below.

The break in the heptad repeat of α/β -peptide **7** takes place at sequence position 23. Leu₂₃, which occupies an *a* position in **4** is displaced from the core by β -ACPC₂₂ which occupies a *d* position in **7**. One turn down the helix, Ile₂₆, which occupies a *d* position in **1**, is still in the hydrophobic core of **7** but now occupies an *a* position. In α/β -peptide **7**, Leu₃₀, which occupies an *a* position in **4** is displaced from the core by Leu₂₉, which occupies a *d* position in **7**. The slight overwinding of the helix bundle resulting from a helical stammer gives rise to one other interesting core packing feature. In proteins, the hydrophobic core position one turn up the helix from a stammer typically forms a hydrophobic core plate that is neither an *a*-layer nor a *d*-layer. This new type of core position, characterized by side chains that are projected directly toward the central axis of the helix bundle, is termed an “*x*-layer” (**1**). β -ACPC₁₉ shows this mode of packing in **7**.

Several factors may contribute to the helical stammer observed in **7**. As discussed in the main text, the substitution of hydrophilic β^3 -Glu₂₂ in **4** with hydrophobic β -ACPC₂₂ in **7** appears to be a key component. In addition, the presence of Leu₂₉, a hydrophobic residue at a noncore *g* position in the GCN4-pLI primary sequence, may also be necessary for the stammer (Leu₂₉ occupies a *d* position in **7**). The shape of the ACPC side chain may make this residue predisposed to occupy an *x*-layer (as it does at position 19 in **7**). We are currently exploring various combinations of acyclic β^3 -residues and cyclic β -residues in the $\alpha\alpha\beta$ backbone shared by α/β -peptides **4** and **7**. We hope that these investigations will provide insight into the origins of the helical stammer in **7** as well as the thermodynamic role of cyclic β -residues in stabilizing the folds of α/β -peptides.

General. Fmoc-protected β^3 -amino acids were purchased from Peptech. The 2,4,6-mesitylene-sulfonyl-3-nitro-1,2,4-triazolide (MSNT), Fmoc-Arg(Pbf) loaded Novasyn TGA resin, unloaded Novasyn TGA resin, and all protected α -amino acids were purchased from Novabiochem. The 2-(1H-benzotriazole-1-yl)-1,1,3,3-tetramethylammonium hexafluoro-phosphate (HBTU) was purchased from AnaSpec. The 1-Methyl-2-pyrrolidinone (NMP) was purchased from Advanced Chemtech. Fmoc-ACPC and Fmoc-APC(Boc) were prepared as previously described (2, 3). Fmoc- β^3 -hArg(Pbf) and Fmoc-APC(Boc) loaded Novasyn TGA resins were prepared by MSNT/1-methylimidazole activation of

the protected amino acid as previously described (4). All other reagents were purchased from Aldrich and used as received unless otherwise noted.

Automated Solid-Phase Peptide Synthesis. Synthesis of α -peptide **1** was carried out on a Symphony Multiple Peptide Synthesizer (Protein Technologies) by using Fmoc-Arg(Pbf) NovaSyn TGA resin. Syntheses of α/β -peptides **2-6** was carried out by using standard Fmoc-solid-phase peptide-synthesis protocols by a combination of manual and automated methods. Novasyn TGA resin preloaded with the C-terminal residue (25 μ mol) was suspended in CH₂Cl₂, allowed to swell for 1 h, and then washed with DMF (three times). The resin was treated with 20% piperidine/DMF (two times for 8 min) to remove the terminal Fmoc group and then washed with DMF (three times). Fmoc-amino acid (75 μ mol) and HBTU (28 mg, 74 μ mol) were weighed into a separate vessel and dissolved in a 0.1 M solution of HOBT in NMP (0.75 ml). DIEA (26 μ l, 150 μ mol) was added, and the solution was allowed to react for 2 min and was then added to the resin. The vessel was capped, placed on a benchtop shaker, and agitated for 1 h. The resin was washed with DMF (three times), and the deprotection/coupling cycle was repeated for the next residue. After coupling of the second residue was complete, the resin was transferred to an Applied Biosystems Synergy 432A automated peptide synthesizer on which the remaining 30 residues were coupled. The N terminus of the resulting α/β -peptide was capped by treatment with 8:2:1 NMP/DIEA/Ac₂O. The resin was washed thoroughly (three times with DMF, three times with CH₂Cl₂, and three times with MeOH) and then dried under vacuum. Peptides were cleaved from resin by treatment with 94:2.5:2.5:1 trifluoroacetic acid (TFA)/H₂O/ethanedithiol/triisopropylsilane. The resin was filtered and washed with additional TFA, and the combined filtrates were concentrated to \approx 2 ml under a stream of dry nitrogen. Crude peptide was precipitated from the cleavage mixture by addition of cold ether (45 ml). The mixture was centrifuged and decanted, and the remaining solid was dried under a stream of dry nitrogen. Purification was carried out as described in *Materials and Methods*.

Microwave-Assisted Manual Solid-Phase Peptide Synthesis. Microwave-assisted reactions were carried out in a MARS multimode microwave reactor (CEM). Novasyn TGA resin preloaded with the C-terminal amino acid (25 μ mol) was weighed into a fritted polypropylene tube and allowed to swell first in CH₂Cl₂ and then in DMF. For coupling of an activated amino acid to an unprotected amine on resin, the desired Fmoc-protected amino acid (125 μ mol) and HBTU (47 mg, 125 μ mol) were dissolved in 1.25 ml of 0.1 M HOBT in DMF. To the solution was added *N*-methylmorpholine (50 μ l, 500 μ mol). This mixture was vortexed briefly and allowed to react for at least 1 min. The activated amino acid solution was then added to the fritted polypropylene tube containing the resin. The resin was heated to 70°C in the microwave (2-min ramp to 70°C, 4-min hold at 70°C) with stirring. After the coupling reaction, the resin was removed from the microwave and washed with DMF (three times), CH₂Cl₂ (three times), and DMF (three times). For Fmoc deprotection, 3 ml of 20% piperidine in DMF was added to the resin, and the mixture was heated to 80°C in the microwave (2-min ramp to 80°C, 2-min hold at 80°C) with stirring. After the deprotection reaction, the resin was washed with DMF (three times), CH₂Cl₂ (three times), and DMF (three times). The cycles of coupling and deprotection were alternately repeated to give the desired full-length peptide. After the final deprotection cycle, the N-

terminal amine was acetylated by stirring the resin in a 14:5:1 mixture of CH_2Cl_2 /acetic anhydride/triethylamine. The resin was washed thoroughly (three times in DMF, three times in CH_2Cl_2 , and three times in MeOH) and then dried under vacuum. Peptides were cleaved from resin by treatment with 94:2.5:2.5:1 trifluoroacetic acid (TFA)/ H_2O /ethanedithiol/triisopropylsilane. The resin was filtered and washed with additional TFA, and the combined filtrates were concentrated to ≈ 2 ml under a stream of dry nitrogen. Crude peptide was precipitated from the cleavage mixture by addition of cold ether (45 ml). The mixture was centrifuged and decanted, and the remaining solid was dried under a stream of dry nitrogen. Purification were carried out as described in *Materials and Methods*.

Analytical Ultracentrifugation Curve Fitting. Apparent molecular mass was determined by nonlinear regression of the equilibrium radial absorbance data by using the program Igor Pro (Wavemetrics). Data were fit to models either for a single species or for equilibrium between monomer and n -mer (Eqs. 1 and 2, respectively):

$$c_r = c_{\text{base}} + c_{\text{ref}} \exp \left[\frac{M(1 - \bar{v}\rho)\omega^2}{2RT} (r^2 - r_{\text{ref}}^2) \right] \quad [1]$$

$$c_r = c_{\text{base}} + c_1 \exp \left[\frac{M_1(1 - \bar{v}\rho)\omega^2}{2RT} (r^2 - r_{\text{ref}}^2) \right] + Kc_1^n \left[\frac{nM_1(1 - \bar{v}\rho)\omega^2}{2RT} (r^2 - r_{\text{ref}}^2) \right]. \quad [2]$$

In Eq. 1, c_r is the concentration of peptide at radial position r , c_{ref} is the concentration of peptide at an arbitrary reference radial position r_{ref} , M is the apparent molecular mass of the peptide, \bar{v} is the partial specific volume of the pep, ρ is the density of the sample, ω is the radial velocity during the measurement, R is the universal gas constant, T is the temperature (in Kelvin), and c_{base} is a correction for baseline absorbance resulting from nonsedimenting components of the sample. The variables in Eq. 2 have the same meaning, except c_1 is the concentration of the monomer, K is the equilibrium constant for the association between the monomer and the n -mer, n is the aggregation number for the species in equilibrium with the monomer, and M_1 is the molecular mass of the monomer.

As a rule, equilibrium sedimentation data were fit to the single-species model first; the equilibrium model was attempted if the single-species fit was unsatisfactory. The quality of a particular fit was judged based on the randomness of residuals and the size of the fit standard deviation. If the single-species and equilibrium models were of similar quality according to these criteria, the simpler model was selected.

As described in the main text, the sedimentation data for peptide **8** at 200 μM peptide concentration in 10 mM NaOAc (pH 4.6) and 150 mM NaCl showed evidence of high-order aggregation. However, the sedimentation data for peptide **8** could be fit to the single species model shown in Eq. 1 when the experiment was performed at a lower peptide concentration (100 μM , **8**) and without NaCl. The following parameters of Eq. 1 were used as constants: $\rho = 0.9975 \text{ g cm}^{-3}$ (tabulated density of 10 mM NaOAc), $\bar{v} = 0.7728 \text{ cm}^3 \text{ g}^{-1}$ (calculated according to the method of Durschlag and Zipper), $c_{\text{base}} = 0.0066$ (the absorbance near the meniscus during the highest speed of the experiment) (5, 6). Global nonlinear regression of the sedimentation data at all experimental speeds gave an apparent molecular mass of 15,390 Da, with a standard deviation of 0.0037 for the fit, and a relatively random distribution of residuals.

The experimental apparent molecular mass is 8% smaller than the molecular mass expected for a tetramer composed of four copies of **8** (16,672 Da). This difference may be a result of charged-based nonideality, in which charge-charge repulsion decreases the apparent molecular mass of peptide assemblies by shifting the radial equilibrium distribution of the peptide away from the bottom of the cell. The difference may also reflect errors in the calculated values of ρ or \bar{v} that were used in the fit. In fact, a 2% increase in either ρ or \bar{v} could account for the deviation of the experimental apparent molecular mass from the calculated molecular mass of the tetramer.

This 8% molecular mass difference could also indicate that peptide **8** is equilibrating between two or more distinct species under the conditions of the experiment. To test this hypothesis, we attempted to fit the sedimentation data for **8** to a monomer-tetramer equilibrium model according to Eq. 2. The same values for ρ , \bar{v} , and c_{base} were used for the equilibrium fit as were used for the single-species fit. Additionally, the following parameters of Eq. 2 were used as constants: $M_1 = 4,168.1 \text{ g mol}^{-1}$ (the molecular mass of peptide **8** monomer), and $n = 4$. The equilibrium constant obtained from this fit is 2152 M^{-3} , suggesting that $\approx 90\%$ of the peptide in a 100 μM solution of **8** would exist as a tetramer, with only 10% as monomer. The residuals and standard deviation (0.0035) of the equilibrium fit are not significantly better than those of the single-species fit; consequently, we did not attempt to fit the sedimentation data for **8** to any additional models of increased complexity (involving more than two equilibrating species, for example).

Both the single-species and equilibrium fits of sedimentation data for peptide **8** lead to the same qualitative conclusion: that **8** forms a stable tetramer in 10 mM NaOAc (pH 4.6) and at 100 μM peptide concentration. The similarity of the residuals and fit standard deviations for each model, and the potential uncertainty that results from nonideality and errors in ρ and \bar{v} preclude a clear choice of which model best describes the sedimentation behavior of peptide **8**. All other things being equal, the simplest model was selected for presentation in the main text.

1. Brown JH, Cohen C, Parry DAD (1996) Heptad breaks in α -helical coiled coils: Stutters and stammers. *Proteins* 26:134–145.
2. Lee HS, LePlae PR, Porter EA, Gellman SH (2001) An efficient route to either enantiomer of orthogonally protected *trans*-3-aminopyrrolidine-4-carboxylic acid. *J Org Chem* 66:3597–3599.
3. LePlae PR, Umezawa N, Lee HS, Gellman SH (2001) An efficient route to either enantiomer of *trans*-2-aminocyclopentanecarboxylic acid. *J Org Chem* 66:5629–5632.
4. Blankemeyer B, Nimtz M, Frank R (1990) An efficient method for anchoring Fmoc-amino acids to hydroxyl-functionalized solid supports. *Tetrahedron Lett* 31:1701–1704.
5. Durschlag H, Zipper P (1994) Calculation of the partial volume of organic compounds and polymers. *Prog Colloid Polym Sci* 94:20–39.
6. Ballerat-Busserolles K, Ford TD, Call TG, Woolley EM (1999) Apparent molar volumes and heat capacities of aqueous acetic acid and sodium acetate at temperatures from $T = 278.15 \text{ K}$ to $T = 393.15 \text{ K}$ at the pressure 0.3(5) MPa. *J Chem Thermodyn* 31:741–762.

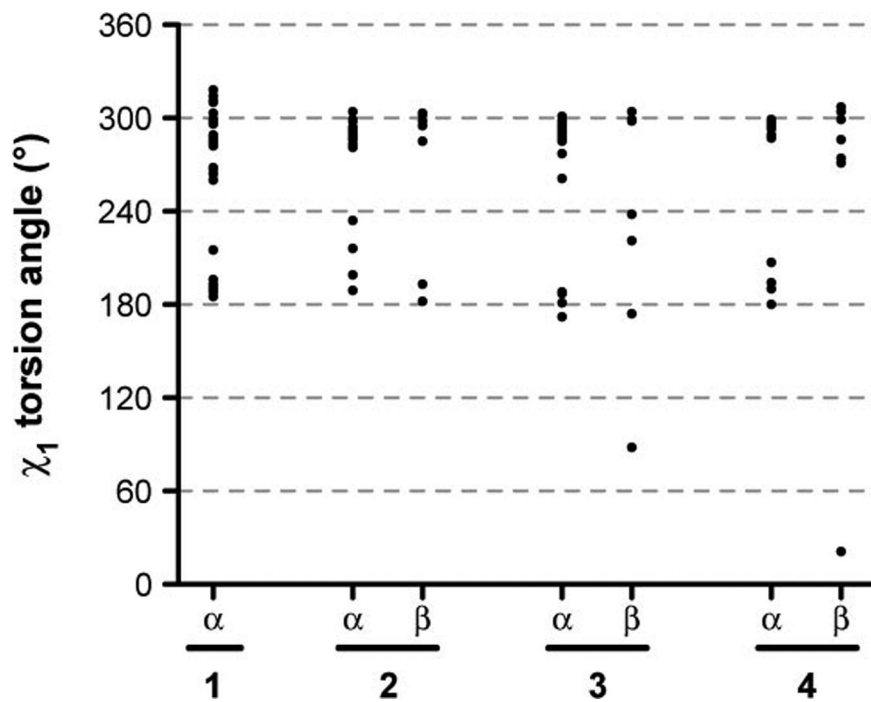


Fig. S1. Plot of χ_1 side-chain torsion angles for α - and β -residues in 1-4.

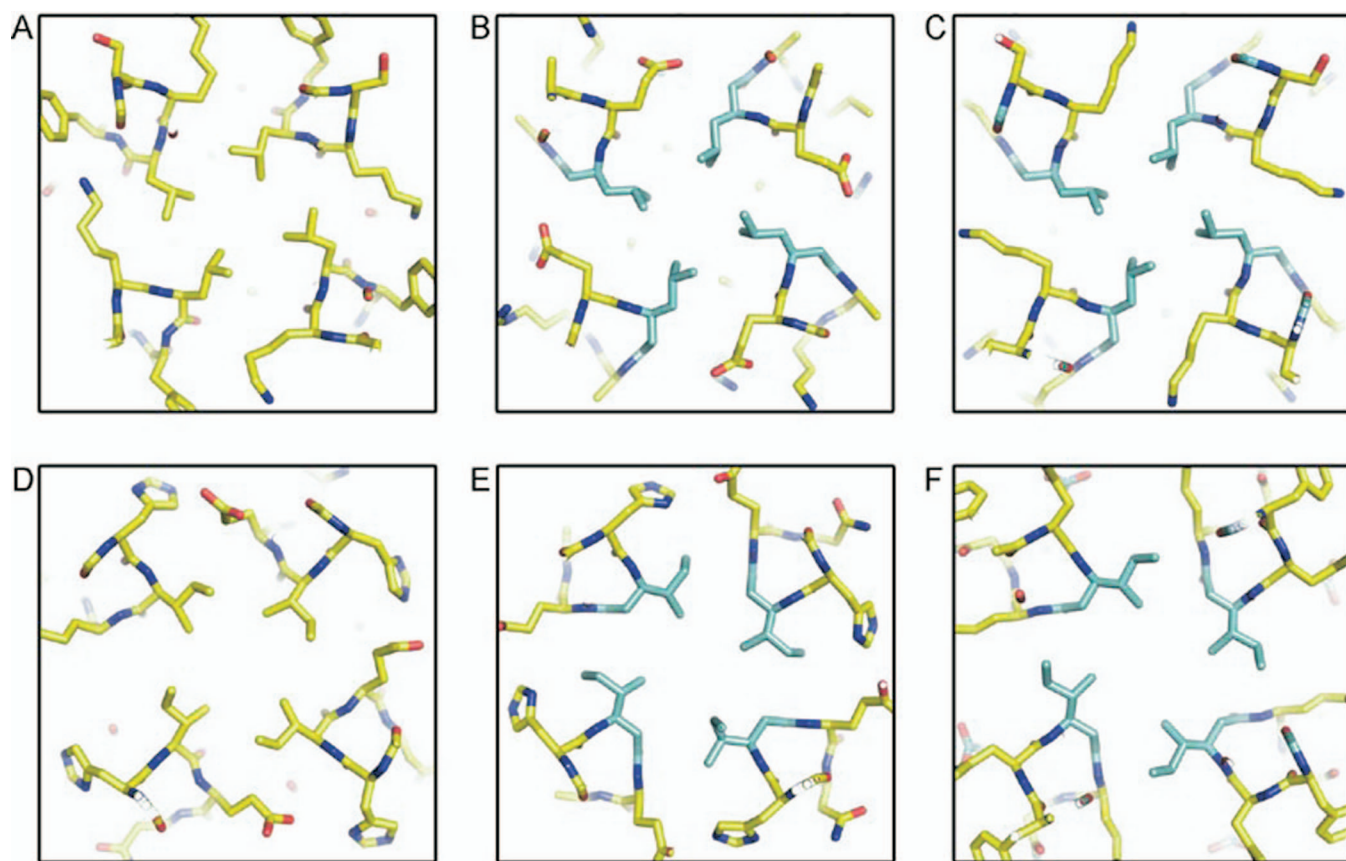


Fig. S2. Comparison of hydrophobic core packing at different residues in α -peptide 1 and α/β -peptides 3 and 4. (A) Leu₁₆ in 1. (B) β^3 -hLeu₂₃ in 3. (C) β^3 -hLeu₁₆ in 4. (D) Ile₁₉ in 1. (E) β^3 -hIle₁₉ in 3. (F) β^3 -hIle₁₉ in 4.

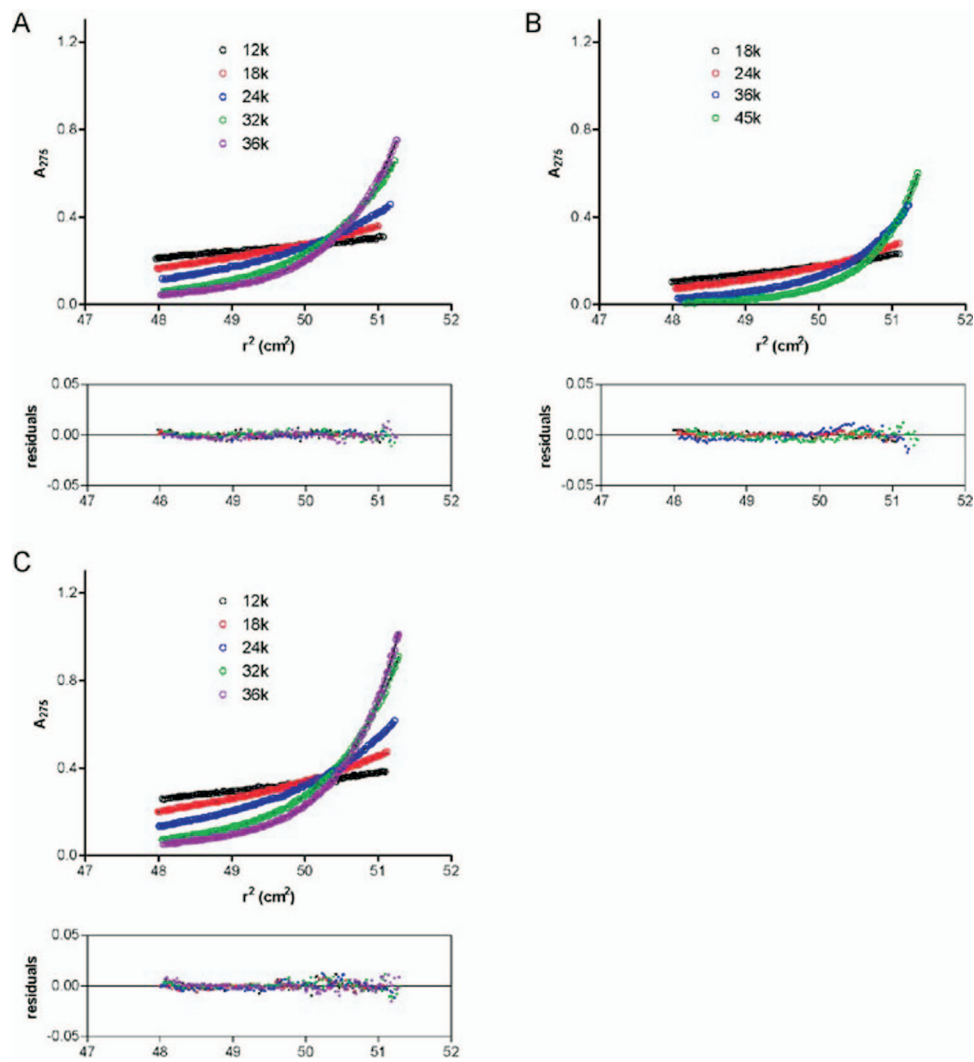


Fig. S6. Analytical ultracentrifugation data with corresponding curve fits and residuals for 7 (A), 8 (B), and 9 (C). α/β -Peptides 7 and 9 are 200 μM in 10 mM NaOAc, 150 mM NaCl (pH 4.6). α/β -Peptide 8 is 100 μM in 10 mM NaOAc (pH 4.6).

Table S1. Crystal data collection and refinement statistics for α/β -peptides 3, 4, and 7

| | 3 | 4 | 7 |
|----------------------------------|-------------|-------------|-------------|
| PDB ID code | 3C3F | 3C3G | 3C3H |
| Data collection | | | |
| Resolution, Å | 47.3–2.0 | 46.5–1.8 | 35.5–2.2 |
| Total observations | 68,825 | 44,471 | 9,836 |
| Unique observations | 7,896 | 3,507 | 1,690 |
| Redundancy | 8.6 (3.0) | 12.5 (3.8) | 5.6 (3.2) |
| Completeness, % | 98.2 (90.1) | 98.5 (92.9) | 98.8 (92.7) |
| I/σ | 17.0 (3.8) | 36.4 (4.4) | 12.6 (3.7) |
| R_{sym}^{\dagger} , % | 7.8 (29.0) | 4.5 (35.8) | 9.8 (30.9) |
| Refinement | | | |
| Resolution, Å | 25.0–2.0 | 25.0–1.8 | 25.0–2.2 |
| R , % | 18.9 | 20.9 | 23.5 |
| $R_{\text{free}}^{\ddagger}$, % | 26.5 | 24.4 | 27.8 |
| Avg. B factor, Å ² | 13.0 | 15.1 | 10.9 |
| RMSD | | | |
| Bonds, Å | 0.011 | 0.015 | 0.016 |
| Angles, ° | 1.7 | 2.1 | 2.2 |

Values in parentheses are for data from the highest-resolution shell (last 0.1 Å interval) in each dataset.

$^{\dagger}R_{\text{sym}} = \sum_n |I_n - \langle I \rangle| / \sum_n I_n$, where I_n is the intensity of an independent observation of reflection n , and $\langle I \rangle$ is the average of multiply recorded and symmetry-related observations of reflection n .

‡ Free R reflections ($\approx 5\%$ of total) were held aside throughout refinement.

Table S2. Calculated helical and superhelical parameters of four-helix bundle folds adopted by GCN4-pLI peptides with different backbone compositions

| | 1 | 2 | 3 | 4 | 7 |
|-----------------------------|--------------|------------------------------------------|-------------------------------|-------------------------|-------------------------|
| Backbone pattern | (α) | ($\alpha\alpha\beta\alpha\alpha\beta$) | ($\alpha\alpha\alpha\beta$) | ($\alpha\alpha\beta$) | ($\alpha\alpha\beta$) |
| Single-helix parameters | | | | | |
| Residues per turn | 3.58 | 3.57 | 3.55 | 3.57 | 3.51 |
| Rise per residue, Å | 1.53 | 1.49 | 1.51 | 1.51 | 1.49 |
| Radius, Å | 2.25 | 2.42 | 2.39 | 2.44 | 2.43 |
| Superhelix parameters | | | | | |
| Supercoil radius, Å | 7.13 | 7.73 | 7.66 | 7.69 | 7.63 |
| Residues per supercoil turn | 129 | 219 | 222 | 185 | 146 |
| Supercoil pitch, Å | 193 | 323 | 331 | 274 | 211 |
| Crossing angle, ° | 26 | 17 | 17 | 20 | 26 |

Values for α -peptide **1** (PDB 1GCL) and α/β -peptide **2** (PDB 2OXX) are calculated from previously published coordinates (refs. 21 and 14, respectively, from the main text).

Table S3. Average backbone dihedral angles for α - and β -residues in 2-4

| | Ideal α -helix | 2 | 3 | 4 |
|--------------------------------|-----------------------|--------------|--------------|--------------|
| α -Residues | | | | |
| $\phi, ^\circ$ | -60 | -66 ± 7 | -67 ± 9 | -67 ± 10 |
| $\psi, ^\circ$ | -50 | -45 ± 7 | -41 ± 6 | -45 ± 7 |
| β -Residues [†] | | | | |
| $\phi, ^\circ$ | - | -111 ± 8 | -106 ± 6 | -111 ± 9 |
| $\theta, ^\circ$ | - | 80 ± 4 | 80 ± 4 | 81 ± 5 |
| $\psi, ^\circ$ | - | -106 ± 5 | -111 ± 3 | -109 ± 6 |

Average and standard deviation for backbone dihedral angles in residues 2-29 are from a single chain in each structure.

[†]Angles ϕ , θ , and ψ for β -residues are defined along N-C $_{\beta}$, C $_{\beta}$ -C $_{\alpha}$, and C $_{\alpha}$ -C $_{\text{carbonyl}}$, respectively.